A Section 508–conformant HTML version of this article is available at https://doi.org/10.1289/EHP4415.

Lipid and Cholesterol Homeostasis after Arsenic Exposure and Antibiotic Treatment in Mice: Potential Role of the Microbiota

Liang Chi,[1] Yunjia Lai,[1] Pengcheng Tu,[1] Chih-Wei Liu,[1] Jingchuan Xue,[1] Hongyu Ru,[2] and Kun Lu[1]

[1]Department of Environmental Sciences and Engineering, University of North Carolina at Chapel Hill, North Carolina, USA
[2]Department of Population Health and Pathobiology, North Carolina State University, Raleigh, North Carolina, USA

Background: Arsenic-induced liver X receptor/retinoid X receptor (LXR/RXR) signaling inhibition is a potential mechanism underlying the cardiovascular effects caused by arsenic. The gut microbiota can influence arsenic toxic effects.

Objective: We aimed to explore whether gut microbiota play a role in arsenic-induced LXR/RXR signaling inhibition and the subsequent lipid and cholesterol dysbiosis.

Methods: Conventional and antibiotic-treated mice (AB-treated mice) were exposed to 0.25 ppm and 1 ppm arsenic for 2 wk. Hepatic mRNAs were extracted and sequenced. The expression levels of genes associated with LXR/RXR signaling were quantified by quantitative real-time polymerase chain reaction (qPCR), and serum and hepatic cholesterol levels were measured. Liquid chromatography–mass spectrometry (LC-MS)–based lipidomics were used to examine serum and hepatic lipids.

Results: Pathway analysis indicated that arsenic exposure differentially influenced the hepatic signaling pathways in conventional and AB-treated mice. The expression of sterol regulatory element-binding protein 1 (*Srebp1c*), 3-hydroxy-3-methylglutaryl-CoA reductase (*Hmgcr*), and cytochrome P450 family 7 subfamily A member 1 (*Cyp7a1*), as well as cholesterol efflux genes, including ATP binding cassette subfamily G member 5/8 (*Abcg5/8*) and cluster of differentiation 36 (*Cd36*), was lower in arsenic-exposed conventional mice but not in AB-treated mice. Similarly, under arsenic exposure, the hepatic expression of scavenger receptor class B member 1 (*Scarb1*), which is involved in reverse cholesterol transport (RCT), was lower in conventional mice, but was higher in AB-treated animals compared with controls. Correspondingly, arsenic exposure exerted opposite effects on the serum cholesterol levels in conventional and AB-treated mice, i.e., higher serum cholesterol levels in conventional mice but lower levels in AB-treated mice than in respective controls. Serum lipid levels, especially triglyceride (TG) levels, were higher in conventional mice exposed to 1 ppm arsenic, while arsenic exposure did not significantly affect the serum lipids in AB-treated mice. Liver lipid patterns were also differentially perturbed in a microbiota-dependent manner.

Conclusions: Our results suggest that in mice, the gut microbiota may be a critical factor regulating arsenic-induced LXR/RXR signaling perturbation, suggesting that modulation of the gut microbiota might be an intervention strategy to reduce the toxic effects of arsenic on lipid and cholesterol homeostasis. https://doi.org/10.1289/EHP4415

Introduction

As a worldwide health problem, arsenic exposure is associated with numerous human diseases, including diabetes, neurological disorders, dermal diseases, and various types of cancer (Naujokas et al. 2013). The relationship between arsenic exposure and cardiovascular diseases (CVDs) has been highly analyzed, and accumulating evidence indicates that arsenic exposure is associated with the increased morbidity and mortality of multiple CVDs, including coronary heart disease, stroke, and atherosclerosis (Navas-Acien et al. 2005; Simeonova et al. 2003; States et al. 2009). For example, a prospective cohort study on 11,746 participants in Bangladesh demonstrated that arsenic exposure was adversely associated with CVD mortality (Chen et al. 2011). Several mechanisms have been proposed to explain arsenic-induced CVDs. For example, several studies suggest that arsenic can promote the development of atherosclerosis by inducing oxidative stress, which promotes inflammatory responses and perturbs endothelial nitric oxide homeostasis (Simeonova and Luster 2004). Liver X receptor/retinoid X receptor (LXR/RXR) signaling can be activated by endogenous ligands, including oxysterols (Mutemberezi et al. 2016) and 9-*cis*-retinoic acid (Willy et al. 1995), to regulate the transcription of numerous genes. Many downstream genes, such as sterol regulatory element-binding protein 1 (*Srebp1c*), ATP binding cassette subfamily A member 1 (*Abca1*), ATP binding cassette subfamily G member 1/5/8 (*Abcg1/5/8*), cluster of differentiation 36 (*Cd36*), and cytochrome P450 family 7 subfamily A member 1 (*Cyp7a1*), play critical roles in cholesterol synthesis, metabolism, and efflux; therefore, members of the LXR/RXR signaling cascade are regarded as cholesterol sensors that control cholesterol levels in tissues (Zhang and Mangelsdorf 2002). In addition, the LXR/RXR signaling axis also influences lipid homeostasis by regulating the expression of related genes (Ulven et al. 2005). For example, previous studies found LXRs can activate the transcription of multiple lipogenic genes like *Srebp1c* and fatty acid synthase (*Fasn*) (Repa et al. 2000; Peet et al. 1998; Joseph et al. 2002a), and consistently, in livers of LXR-deficient mice, these genes have low expression levels (Peet et al. 1998; Repa et al. 2000). Moreover, a previous study demonstrated that a synthetic LXR ligand reduced atherosclerotic lesions in two mouse models (Joseph et al. 2002b), suggesting that activation of the LXR/RXR pathway may attenuate atherosclerosis, and by extension, that the LXR/RXR signaling may play a role in the development of CVDs in general. Recent studies revealed that the LXR/RXR signaling pathway was inhibited by arsenic exposure (Padovani et al. 2010), which was directly associated with arsenic-induced atherosclerosis in an apolipoprotein E knockout ($ApoE^{-/-}$) mouse model (Lemaire et al. 2014). Previous studies have shown that arsenic exposure inhibits the expression of genes downstream of the LXR/RXR signaling pathway, such as *Abca1* and *Srebp1c* (Lemaire et al. 2011; Padovani et al. 2010), and LXRα knockout prevents arsenic-enhanced atherosclerosis in $ApoE^{-/-}$ mice (Lemaire et al. 2014). These findings suggested that perturbation of the LXR/RXR signaling axis potentially represents an important mechanism underlying the cardiovascular effects of arsenic.

Address correspondence to Kun Lu, MHRC 0031, 135 Dauer Drive, UNC-Chapel Hill, 27599. Email: Kunlu@unc.edu

Supplemental Material is available online (https://doi.org/10.1289/EHP4415).

The authors declare they have no actual or potential competing financial interests.

Received 31 August 2018; Revised 5 August 2019; Accepted 13 August 2019; Published 18 September 2019.

Note to readers with disabilities: *EHP* strives to ensure that all journal content is accessible to all readers. However, some figures and Supplemental Material published in *EHP* articles may not conform to 508 standards due to the complexity of the information being presented. If you need assistance accessing journal content, please contact ehponline@niehs.nih.gov. Our staff will work with you to assess and meet your accessibility needs within 3 working days.

The gut microbiota is deeply involved in numerous host physiological processes, such as food digestion, immune system development, and xenobiotic biotransformation (Jandhyala et al. 2015; Nicholson et al. 2012), and also plays an important role in the development of CVDs. For example, the gut microbiota–produced trimethylamine (TMA) can be oxidized to TMA oxide (al-Waiz et al. 1992; Romano et al. 2015), which enhanced macrophage cholesterol accumulation (Wang et al. 2011) and induced the development of atherosclerotic plaques (Koeth et al. 2013) in mouse models. Moreover, gut microbiota–stimulated inflammation can modulate host gene expression to affect lipid and cholesterol homeostasis, which increases the risk of atherosclerosis (Caesar et al. 2010). Recently, studies have shown that complex interactions exist between arsenic exposure and the gut microbiota. On the one hand, arsenic exposure can perturb the normal gut microbiota community and alter its metabolic pattern (Chi et al. 2017; Lu et al. 2014a); on the other hand, the gut microbiota also influences arsenic biotransformation and its toxic effects (Chi et al. 2018; Lu et al. 2014b; Rubin et al. 2014). However, whether the gut microbiota influences arsenic-induced LXR/RXR inhibition and cholesterol/lipid dysbiosis remains unknown. In this study, we treated mice with antibiotics to generate a mouse model with the gut microbiota being largely reduced or depleted, and compared the effects of arsenic exposure on LXR/RXR signaling and cholesterol and lipid homeostasis in conventional mice and mice treated with antibiotics.

Methods

Animals, Gut Microbiota Depletion, Arsenic Exposure, and Sample Collection

Sodium arsenite was obtained from Fisher Scientific, and 60 C57BL/6 female mice (specific pathogen-free grade, approximately 7 wk old) were purchased from Jackson Laboratories. All mice were maintained at the University of North Carolina animal facility in static microisolator cages with Bed-O-Cob (The Andersons Inc., Maumee, OH) combination bedding under standard environmental conditions (22°C, 40–70% humidity, and a 12:12-h light: dark cycle). Before the experiment began, the mice were observed for 1 wk at the animal facility. Figure 1A shows the workflow of this study. Briefly, 30 mice were each treated with either antibiotics [cefoperazone (0.5 mg/mL); Sigma-Aldrich] via drinking or clean drinking water for 72 h before arsenic exposure to generate the gut microbiota–depleted mouse model (AB-treated mouse) (Antonopoulos et al. 2009; Theriot et al. 2016) and conventional mouse control groups, respectively. Then, mice were divided into six groups (10 mice each) as follows: Group #A: conventional mouse control group; Group #B: conventional mice exposed to 0.25 ppm arsenic for 2 wk via their drinking water; Group #C: conventional mice exposed to 1 ppm arsenic for 2 wk via their drinking water; Group #D: AB-treated mouse control group; Group #E: AB-treated mice exposed to 0.25 ppm arsenic for 2 wk via their drinking water; and Group #F: AB-treated mice exposed to 1 ppm arsenic for 2 wk via their drinking water. The 0.25 ppm arsenic is a relevant human dose level, and some arsenic-contaminated areas were reported that contained 0.25 ppm or higher levels of arsenic in the water, such as Bangladesh (Chowdhury et al. 2000), India (Singh 2004), and Vietnam (Berg et al. 2001), and 1 ppm arsenic also can be found in the groundwater in some severely contaminated areas (Berg et al. 2001). Both 0.25-ppm and 1-ppm dose levels have been widely adopted by previous studies (Cui et al. 2006; Hong et al. 2009; Straub et al. 2007). Standard pelleted rodent diet and sterilized tap water were provided to the mice *ad libitum*. Drinking water was refreshed twice a week, and weekly water consumption of each cage (five mice per cage) was monitored (Table S2). The antibiotics were administered to AB-treated mice throughout the arsenic exposure to maintain the gut microbiota depletion condition. After 2 wk of arsenic exposure, the mice were euthanized with carbon dioxide and necropsied to collect their sera and livers. Heart blood were collected, put in blood collection tubes (BD Microtainer®; BD), and centrifuged at $10{,}000 \times g$ at room temperature for 1 min after 1 to 2 h. Then, sera (the upper layer) were collected and stored in −80°C until use. Half of each liver was placed in liquid nitrogen, and the other half was treated with RNA*later* (Thermo Fisher Scientific) for gene expression analysis. All samples were stored at −80°C until use. All mice were treated humanely, and the experimental protocol was approved by the University of North Carolina Animal Care Committee.

Validation of Gut Microbiota Depletion by Antibiotics

After 72 h antibiotics treatment, we collected mouse fecal samples and extracted fecal DNA using a PowerSoil® DNA Isolation Kit (Qiagen) according to instructions of the manufacturer. A negative control was set by adding no fecal sample in each batch of DNA extraction. DNA samples were quantified by a NanoDrop spectrophotometer (Thermo Fisher Scientific), and then we amplified bacterial 16S ribosomal ribonucleic acid (rRNA) with universal primers (iTRU-A 515 F and iTRU-1 806 R) by polymerase chain reaction (PCR) on a C1000 Touch™ thermal cycler (Model 550; Bio-Rad) programmed as follows: 3 min at 95°C for initial denaturation and 18 cycles of 20 s at 95°C, an annealing step at 60 °C for 30 s, 30 s at 72°C for extension, and 5 min at 72°C for a final extension, as previously described (Lu et al. 2014a). PCR products were loaded to a 1.5% agarose gel to perform gel electrophoresis, and the signal intensities were checked under ultraviolet (UV) light.

Liver RNA-Seq Library Preparation, Sequencing, and Data Analysis

The RNeasy Mini Kit (Qiagen) was used to isolate RNA from the liver (conventional control, 0.25 ppm arsenic-treated conventional mice, AB-treated mice, and 0.25 ppm arsenic- and AB-treated mice) according to the manufacturer's instructions. The resulting RNA was then digested with a DNA-free™ DNA Removal Kit (Thermo Fisher Scientific) to remove genomic DNA contaminants. The RNA quality was assessed on an Agilent 4200 TapeStation (Agilent Technologies), and the RNA integrity number threshold was set to 8.5. The KAPA stranded mRNA-Seq (transcriptome sequencing) kit (Kapa Biosystems) was used to prepare the RNA-Seq library according to the manufacturer's protocol. The libraries were sequenced at the Georgia Genomics Facility using an Illumina NextSeq High Output Flow Cell, and approximately 10 million reads were generated for each sample. Sequencing data were uploaded to the galaxy server (https://usegalaxy.org/), HISAT2 (Galaxy Version 2.1.0+galaxy4) (Kim et al. 2015) was applied to align the results, and Cufflinks (Galaxy Version 2.2.1.2) and Cuffdiff (Galaxy Version 2.2.1.5) were applied to assemble the transcripts, estimate their abundances, and detect significant changes in transcript expression (Trapnell et al. 2010). The differential gene expression table were uploaded to Qiagen's Ingenuity® Pathway Analysis (IPA®; Qiagen) software for pathway analysis. The cutoff value for each gene was set as $q < 0.05$. Top canonical pathways (top five pathways with the smallest p-values) generated by IPA were analyzed, and z-scores were automatically calculated by IPA.

Quantitative Real-Time Polymerase Chain Reaction

The hepatic RNAs of all six groups of mice ($n = 8$/group) were extracted by the RNeasy Mini Kit (Qiagen) following the

manufacturer's instructions. The digestion of potential contaminated genomic DNA was performed as described above. cDNA was synthesized using iScript™ Reverse Transcription Supermix (Bio-Rad Laboratories), and the sixfold diluted products were used for quantitative real-time PCR (qPCR). qPCR was performed on a Bio-Rad CFX96 Touch Real-Time PCR Detection System using SsoAdvanced™ Universal SYBR® Green Supermix (Bio-Rad). The qPCR conditions were 95°C for 10 min, followed by 39 cycles of 15 s at 95°C, 30 s of annealing at primer-specific temperatures, and 30 s at 72°C, and a final melting curve analysis was performed by raising the temperature from 65–95°C in 0.5°C increments for 0.05 s each. The sequences of the primers (purchased from Integrated DNA Technologies) and their annealing temperatures used for qPCR are shown in Table S1. β-actin was used as the endogenous control, and the relative expression of each gene was calculated using the ΔΔCT method with CFX (version 3.1) manager software (Bio-Rad). The No-RT control and No-template control were set to avoid potential genomic DNA contamination and other technical contaminants, which were run in exactly the same way as the experimental samples but replaced reverse transcriptase solution and templates with nonreverse transcriptase solution and water, respectively.

Liver and Serum Total Cholesterol Measurement

Liver and serum total cholesterol levels were measured using a cholesterol assay kit [Cholesterol Assay Kit - high-density lipoprotein (HDL) and low-density lipoprotein (LDL)/very low-density lipoprotein (VLDL) (ab65390); Abcam]. The colorimetric assay protocol was used, and the detection range was from 0 to 100 ng/μL. All experimental procedures were performed according to the manufacturer's protocol.

Liver and Serum Lipid Extraction, Liquid Chromatography–Mass Spectrometry Measurement, and Data Analysis

Liver and serum lipid extraction was performed according to a previously described method with some modifications (Matyash et al. 2008). Briefly, for serum, a 20-μL sample aliquot was placed in a 1.5-mL Eppendorf tube, 225 μL of cold methanol was added, and the sample was vortexed for 10 s. For the liver, 50 mg sample was placed in a 1.5-mL Eppendorf tube containing 2.8-mm zirconium oxide beads, 225 μL of cold methanol was added, and the sample was homogenized on a TissueLyzer (Qiagen, Hilden, German) at 50 Hz for 10 min. Then, for both liver and serum samples, 750 μL of cold methyl tert-butyl ether was added, and the sample was shaken on an orbital mixer for 10 min. Next, 188 μL of room-temperature liquid chromatography–mass spectrometry (LC-MS)–grade water was added, and the sample was vortexed for 20 s. The sample was centrifuged at 14,000 × *g* for 2 min, and approximately 700 μL of liquid was transferred from the top layer, dried in a SpeedVac (Thermo Fisher Scientific, Waltham, MA), and reconstituted in 65 μL of methanol: chloroform (90:10, v/v) for instrumental analysis. The serum and liver lipids were analyzed on an Agilent 6530Accurate Mass Quadrupole Time-of-Flight (Q-TOF) LC/MS system (Agilent) in negative and positive modes with a full scan mode. The MS1 data files were uploaded to the XCMS online server (https://xcmsonline.scripps.edu/) to align the peaks and calculate the peak intensities. The ultra-performance liquid chromatography (UPLC)/Q-TOF parameter set was selected. The significantly changed features were selected ($q < 0.05$; intensity >1,000), and METLIN (Scripps Research) and LIPID MAPS (https://www.lipidmaps.org/) were used to annotate peaks (*m/z* accuracy was set to 10 ppm).

Statistical Analysis

Differential gene expressions for RNA-Seq data were determined by Cuffdiff in galaxy, and $q < 0.05$ was set as the threshold. The two-way analysis of variance (ANOVA) in Prism 8 software (GraphPad) was applied to determine the statistical significance of gene expression differences measured by quantitative real-time reverse transcription PCR (qRT-PCR) and the different levels of hepatic and serum cholesterol. When two-way ANOVA reported the interaction *p*-value to be less than 0.05, Dunnett's multiple comparisons test was performed to determine how arsenic exposure changed the gene expression or cholesterol level. All adjusted *p*-values were calculated in Dunnett's multiple comparisons test in Prism 8 software. The specific calculating equations are as follows:

$$MS\,(\text{Error}) = MS\,(\text{Subject} \times \text{Row factor})$$

$$\text{Mean diff} = \text{Mean}\,(\text{group1}) - \text{Mean}\,(\text{group2})$$

$$SE\,\text{Difference} = \sqrt{MS\,(\text{Error}) * \left(\frac{1}{N1} + \frac{1}{N2}\right)}$$

$$q = \frac{|\text{Mean diff}|}{SE\,\text{Difference}}$$

$$\text{Adjusted } p\text{-value} = \text{PFromQDunnet}(q, DF, M).$$

where $N1$ and $N2$ are the sample sizes of group1 and group2, respectively; $MS\,(\text{Error})$ is the appropriate mean square error; and Mean diff is the mean difference between two groups.

An adjusted *p*-value (calculated by Prism 8 software) of less than 0.05 was considered a significant difference. For the LC-MS–based lipidomics, the featured differences between the two groups were determined by the unpaired parametric Welch's *t*-test, and the *q*-value threshold was set to 0.05.

Results

Effects of Antibiotics on Depleting Gut Bacteria and Water Consumption in Mice

DNA quantities from the fecal samples of AB-treated mice were extremely low, as measured by a NanoDrop spectrophotometer, suggesting no significant amount of bacterial DNA could be extracted from AB-treated samples (fecal DNA concentration of conventional mice: 63.0 ± 31.2 ng/μL; fecal DNA concentration of AB-treated mice: 0.1 ± 0.3 ng/μL). Next, we used primers specific to the V4 region of bacterial 16S gene to amplify the sample for 18 cycles, followed by electrophoresis and visualization by UV light. No signal could be detected in the PCR products of AB-treated mice, while fecal samples from conventional mice had good 16S rRNA gene signals according the electrophoresis results (Figure S1). Therefore, these results demonstrated that antibiotics treatment significantly reduced or depleted gut bacteria in mice. In addition, we did not observe a water consumption difference between conventional mice and AB-treated mice (Table S2).

Effect of Arsenic Exposure on Hepatic Signaling Pathways in Conventional and Antibiotic-Treated Mice

As a preliminary test to examine potential differential gene expressions, we first performed hepatic mRNA sequencing to compare the 0.25 ppm arsenic-induced differential gene expression in conventional and AB-treated mice, and we analyzed the disturbed metabolic pathways with IPA software. As shown in

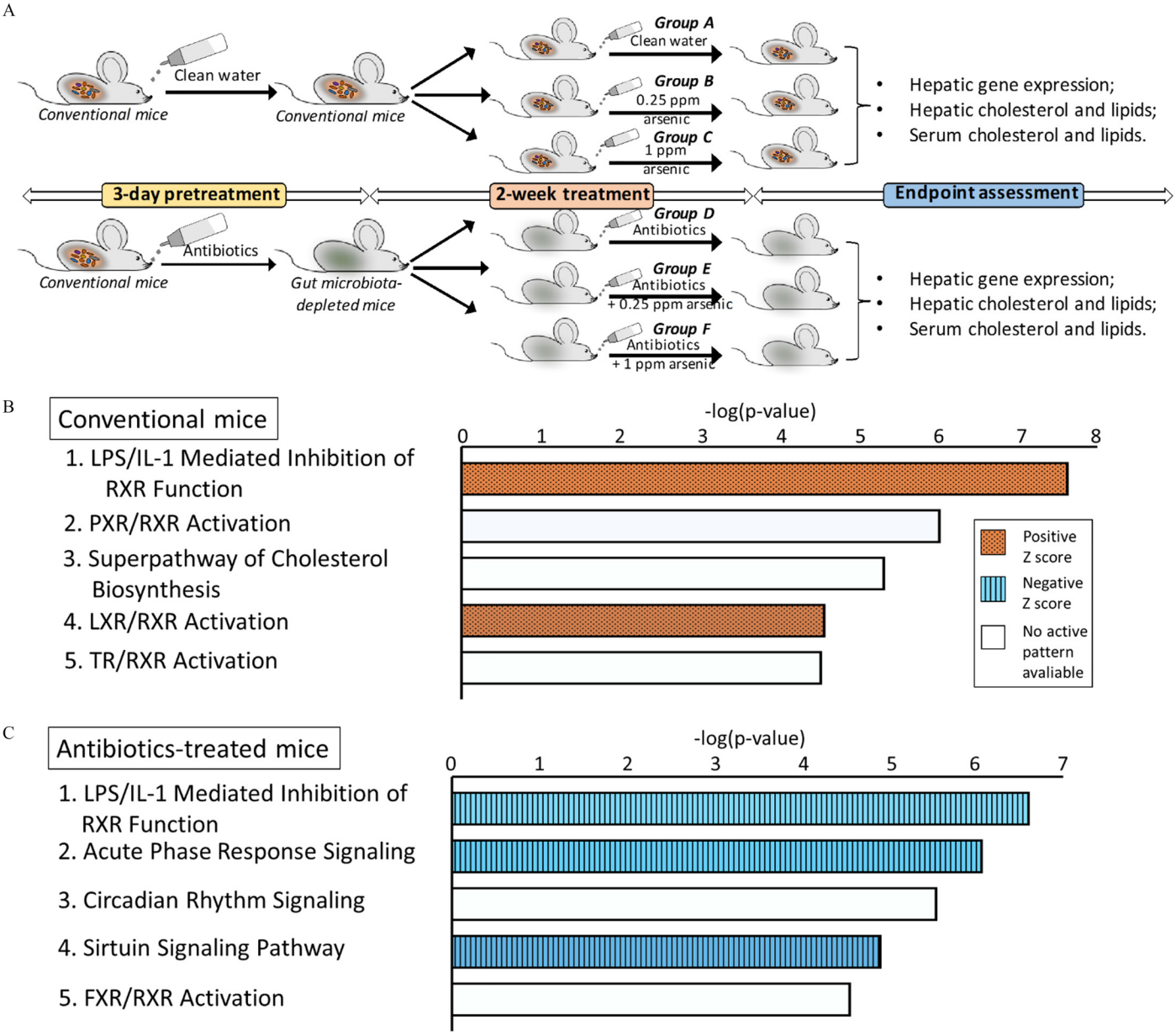

Figure 1. The experimental workflow and RNA-Seq (transcriptome sequencing) pathways. (A) Experimental workflow. (B,C) The top canonical pathways altered by arsenic exposure in livers of conventional and antibiotic (AB)-treated mice, respectively ($n = 5$/group). Note: IL-1, interleukin 1; LPS, lipopolysaccharide; PXR, pregnane X receptor; RXR, retinoid X receptor.

Figure 1B,C, in the top canonical pathways (with the smallest *p*-values), the "LPS/IL-1 Mediated Inhibition of RXR Function" pathway was oppositely regulated by arsenic exposure in conventional and AB-treated mice. In addition, the enrichment of various RXR-related pathways was significantly perturbed in the 0.25 ppm arsenic-treated conventional mice, especially the LXR/RXR signaling pathway (Figure 1B). Moreover, the cholesterol biosynthesis was one of the top five pathways perturbed by arsenic exposure in conventional mice but not in AB-treated mice (Figure 1B,C; Tables S3 and S4). Likewise, the mRNA associated with the "Acute phase response signaling" and "Sirtuin signaling" pathways were in the top five pathways in AB-treated mice dosed with arsenic, but not in conventional mice. Major genes with differential expression levels between the two groups in each pathway are summarized in Tables S3 and S4.

Effects of Arsenic on the Expression of Downstream LXR/RXR Genes Associated with Cholesterol Metabolism and Efflux in Conventional and Antibiotic-Treated Mice

Based on the RNA-Seq results, we hypothesized that arsenic exposure exerts different effects on hepatic LXR/RXR signaling as well as on cholesterol homeostasis in conventional and AB-treated mice. We applied qPCR to examine the expression of genes downstream of the LXR/RXR signaling pathway in livers of the two types of mice. Compared with the vehicle-treated mice, expression of multiple genes downstream of the LXR/RXR signaling pathway was significantly lower in both the 0.25-ppm and 1-ppm arsenic-exposed conventional mice groups, as were genes related to cholesterol homeostasis (Figures 2 and 3). First, genes associated with cholesterol synthesis and metabolism, including *Srebp1c* (Figure 2A), 3-hydroxy-3-methylglutaryl-CoA

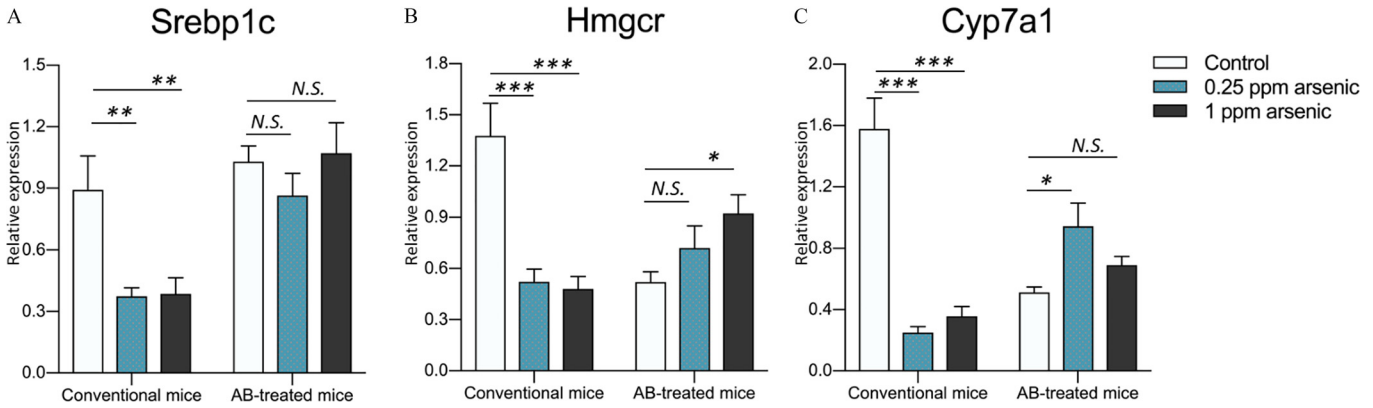

Figure 2. (A) Hepatic expression of sterol regulatory element-binding protein 1 (*Srebp1c*), (B) 3-hydroxy-3-methylglutaryl-CoA reductase (*Hmgcr*), and (C) cytochrome P450 family 7 subfamily A member 1 (*Cyp7a1*) in conventional and antibiotic (AB)-treated mice. Mice treated with either water or 0.5 mg/mL cefoperazone were exposed to either vehicle, 0.25 ppm arsenic, or 1.0 ppm arsenic for 2 wk, after which mice were euthanized and liver tissues were harvested. Hepatic expression was evaluated using quantitative real-time reverse transcription polymerase chain reaction (qRT-PCR). Graphs show mean expression relative to endogenous control (β-actin) + standard error of the mean (±SEM). $n = 6$–8 per group. N.S., no significant difference ($p > 0.05$); $^{*}p < 0.05$; $^{**}p < 0.01$; $^{***}p < 0.001$. Adjusted *p*-values were determined by two-way analysis of variance (ANOVA) Dunnett's multiple comparisons test.

reductase (*Hmgcr*) (Figure 2B), and *Cyp7a1* (Figure 2C), were expressed significantly less in arsenic-exposed conventional mice compared with controls. By contrast, in the AB-treated groups, the expression levels of *Hmgcr* (in mice treated with 1 ppm arsenic) and *Cyp7a1* (in mice treated with 0.25 ppm arsenic) were significantly higher than those in the AB-treated control group, while the expression of *Srebp1c* was not significantly different among the different treatment groups (Figure 2). In

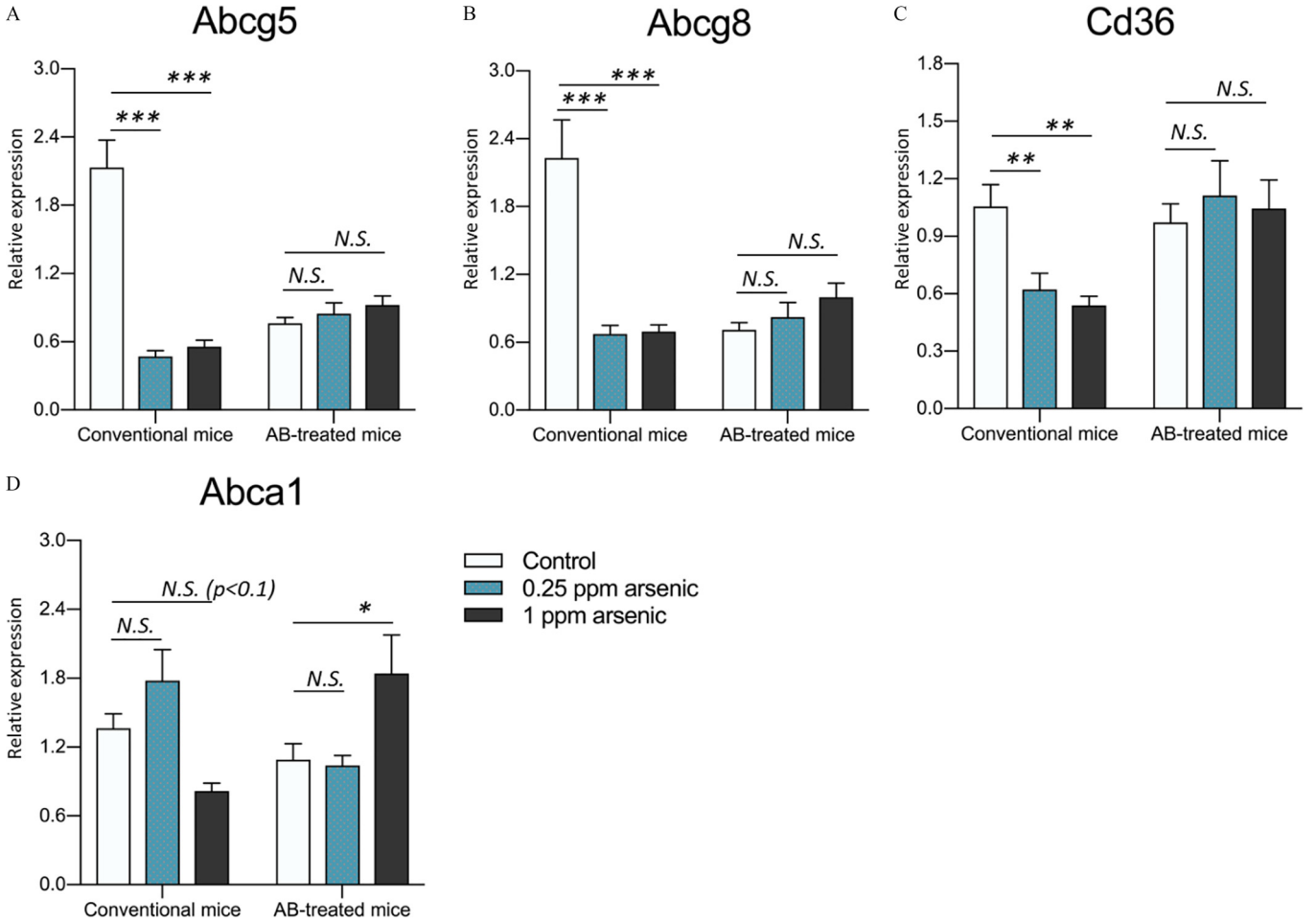

Figure 3. (A) Hepatic expression of ATP binding cassette subfamily G member 5/8 (*Abcg*5), (B) *Abcg8*, (C) cluster of differentiation 36 (*Cd36*), and (D) ATP binding cassette subfamily A member 1 (*Abca1*) in conventional and antibiotic (AB)-treated mice. Mice treated with either water or 0.5 mg/mL cefoperazone were exposed to either vehicle, 0.25 ppm arsenic, or 1.0 ppm arsenic for 2 wk, after which mice were euthanized and liver tissues were harvested. Hepatic expression was evaluated using quantitative real-time reverse transcription polymerase chain reaction (qRT-PCR). Graphs show mean expression relative to endogenous control (β-actin) + standard error of the mean (SEM). $n = 6$–8 per group. N.S., no significant difference ($p > 0.05$); $^{*}p < 0.05$; $^{**}p < 0.01$; $^{***}p < 0.001$. Adjusted *p*-values were determined by two-way analysis of variance (ANOVA) Dunnett's multiple comparisons test.

addition, multiple cholesterol efflux-associated genes, including *Abcg5* (Figure 3A), *Abcg8* (Figure 3B), and *Cd36* (Figure 3C), were also expressed at lower levels in arsenic-treated conventional mice than in the controls. However, none of the expression of these genes was significantly different in arsenic-exposed AB-treated animals compared with vehicle-exposed AB-treated animals (Figure 3). Also, compared with controls, 1 ppm arsenic exposure resulted in moderately lower (adjusted $p < 0.1$) expression of *Abca1* in conventional mice, but significantly higher expression in AB-treated mice (Figure 3D). Specific two-way ANOVA and multiple-comparison test results are shown in Tables S5 and S6.

Effects of Arsenic on the Expression of Downstream LXR/RXR Genes Associated with Markers of Reverse Cholesterol Transport in Conventional and Antibiotic-Treated Mice

Genes associated with reverse cholesterol transport (RCT) were also differentially expressed in mice treated with antibiotics compared with those that were not. In conventional animals, hepatic expression of scavenger receptor class B member 1 (*Scarb1*) was significantly lower after treatment with arsenic than in controls (Figure 4B). However, expression of both LDL receptor (*Ldlr*) and *Scarb1* was significantly higher in AB-treated mice exposed to 1 ppm arsenic than in AB-treated controls (Figure 4A,B).

Serum and Hepatic Cholesterol Concentrations in Conventional and AB-Treated Mice Exposed to Arsenic

To further validate our hypothesis, we measured the cholesterol concentrations in the serum and liver. As shown in Figure 5A, the serum cholesterol concentrations in 1 ppm arsenic-exposed conventional mice were significantly higher than those in control mice. By contrast, in AB-treated mice, the serum cholesterol level was significantly lower after 1 ppm arsenic exposure (Figure 5A). Furthermore, serum cholesterol levels in 0.25 ppm arsenic-exposed animals were not significantly different compared with vehicle-exposed animals, but we still observed that serum cholesterol concentrations in 0.25 ppm arsenic-exposed conventional mice were moderately higher (adjusted $p > 0.05$) than those in control mice, while they were moderately lower (adjusted $p > 0.05$) in 0.25 ppm-treated and AB-treated mice than in AB-treated mice (Figure 5A). In addition, hepatic cholesterol levels in arsenic-exposed mice were not significantly different in either conventional mice or AB-treated mice compared with vehicle controls (adjusted $p > 0.05$; Figure 5B).

Serum and Hepatic Lipid Patterns in Conventional and Antibiotic-Treated Mice Exposed to Arsenic

We next investigated whether the effects of arsenic exposure on lipid homeostasis differed between conventional and AB-treated mice, using the 1-ppm arsenic group as an example. Figure 6 shows the serum lipids significantly perturbed by arsenic exposure in conventional mice. Dramatically, the levels of numerous triglycerides (TGs) were significantly higher in arsenic-treated conventional mice than in controls. Moreover, the levels of multiple lipids in sera were higher in arsenic-treated conventional mice than in controls, including phosphatidylserine, phosphatidylglycerol (PG), phosphatidylethanolamine (PE), phosphatidic acid (PA), and diacylglycerol (DG). However, no lipid feature has significant difference between control and 1-ppm arsenic-treated mice under antibiotic treatment conditions.

In the liver, similarly, we found that the level of numerous lipids in conventional mice were disturbed by 1 ppm of arsenic exposure (Figure 7). The levels of many monoacylglycerols (MGs) were higher in arsenic-treated conventional mice than in controls, while the levels of most of the perturbed PAs, Pes, and PGs were lower. However, for AB-treated mice, we did not detect any hepatic lipid to have significant difference between controls and arsenic-treated mice.

Discussion

In this study, we investigated the roles of the gut microbiota on the arsenic-induced down-regulation of LXR/RXR signaling. The LXR/RXR signaling axis plays a central regulatory role in numerous physiological processes and especially affects lipid and cholesterol homeostasis (Mutemberezi et al. 2016; Ulven et al. 2005; Willy et al. 1995; Zhang and Mangelsdorf 2002). Previous studies demonstrated that arsenic exposure affects the expression of genes downstream of the LXR/RXR signaling cascade. For

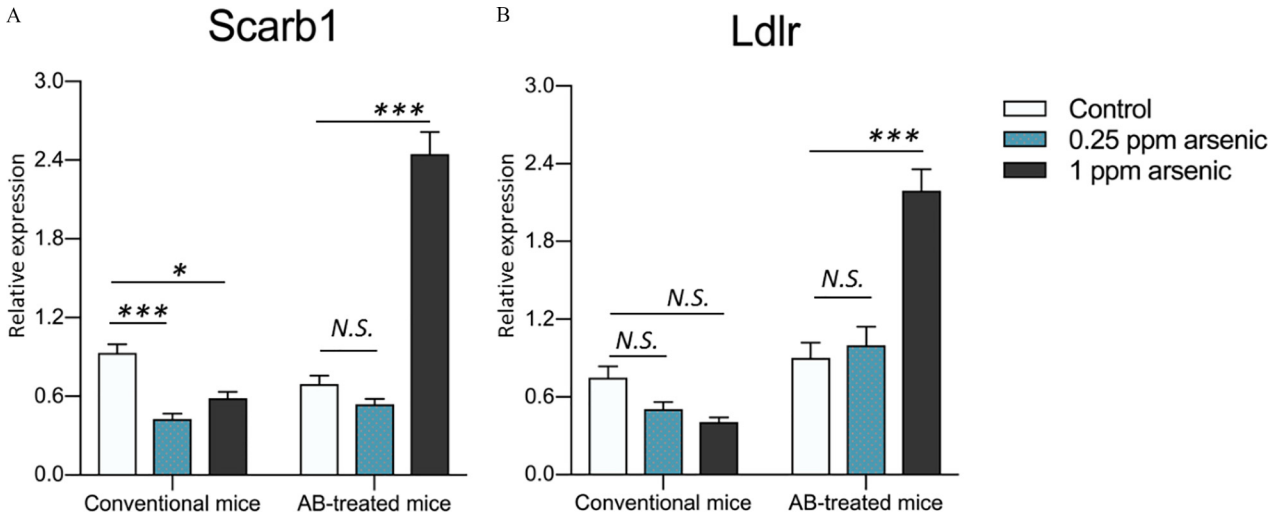

Figure 4. (A) Hepatic expression of scavenger receptor class B member 1 (*Scarb1*) and (B) low-density lipoprotein receptor (*Ldlr*) in conventional and antibiotic (AB)-treated mice. Mice treated with either water or 0.5 mg/mL cefoperazone were exposed to either vehicle, 0.25 ppm arsenic, or 1.0 ppm arsenic for 2 wk, after which mice were euthanized and liver tissues were harvested. Hepatic expression was evaluated using quantitative real-time reverse transcription polymerase chain reaction (qRT-PCR). Graphs show mean expression relative to endogenous control (β-actin) + standard error of the mean (SEM). $n = 6$–8 per group. N.S., no significant difference ($p > 0.05$); $^{*}p < 0.05$; $^{***}p < 0.001$. Adjusted p-values were determined by two-way analysis of variance (ANOVA) Dunnett's multiple comparisons test.

example, arsenic exposure could reduce the LXR/RXR ligand-induced expression of *Abca1* and *Srebp1c* in macrophages (Padovani et al. 2010). In addition, 5 wk of 0.1 ppm arsenic exposure inhibited the mouse hepatic expression of *Srebp1c* (Adebayo et al. 2015). Moreover, in the *ApoE*$^{-/-}$ mouse model, arsenic exposure increased atherosclerosis, potentially by inhibiting LXR/RXR target genes, and LXRα knockout attenuated the effects of arsenic on atherosclerosis (Lemaire et al. 2011, 2014). In this study, we also found that arsenic exposure disturbed the LXR/RXR signaling axis (Figure 1). The lower expression levels of multiple genes downstream of the LXR/RXR signaling cascade suggest that this pathway is inhibited by arsenic treatment (Figures 2 and 3). However, arsenic-induced LXR/RXR signaling inhibition was not observed in AB-treated mice, which suggests the important role of a normal gut microbiota in the effects of arsenic on hepatic LXR/RXR signaling.

Previous studies suggest that arsenic exposure influences cholesterol homeostasis. For example, an early study demonstrated that arsenic exposure can increase the total serum cholesterol levels in humans (Auken 1945), and another study found that arsenic inhibited the LXR/RXR signaling pathway to decrease *Abca1* expression, which inhibited cholesterol efflux from human and murine macrophages (Padovani et al. 2010). Here, we found that compared with vehicle, arsenic exposure resulted in lower expression of multiple genes related to cholesterol synthesis and metabolism in the liver, such as *Srebp1c, Hmgcr*, and *Cyp7a1* (Figure 2), and the liver is the main location in which cholesterol synthesis occurs. As a transcription factor, *Srebp1c* can be induced by LXR/RXR signaling to induce the transcription of genes associated with fatty acid and cholesterol synthesis (Repa et al. 2000; Shimano 2001). In addition, *Hmgcr* encodes the rate-limiting enzyme in cholesterol synthesis pathways, and *Cyp7a1* encodes the rate-limiting enzyme of bile acid synthesis (Chiang et al. 2001; Pandak et al. 2001; Sharpe and Brown 2013). Therefore, arsenic-decreased expression of these genes should disturb cholesterol homeostasis. However, despite the lower expression of cholesterol synthesis genes, the concentration of hepatic cholesterol in arsenic-exposed animals was not significantly different (Figure 5B). This result could partially be due to the lower expression of *Cyp7a1*, which reduces the cholesterol conversion to bile acids (Figure 2A). In addition, the low expression of *Abcg5* and *Abcg8* might also compensate for the decrease in cholesterol synthesis (Figure 3), since they effluxed cholesterol from the liver to peripheral tissues (Attie 2007; Yu et al. 2014). By contrast, the expression of these genes in arsenic-exposed mice treated with antibiotics was often not significantly different from control or, in some cases, was significantly different, but in a direction opposite that of the conventional mice (Figures 2 and 3). These data suggest that the reduction or depletion of the gut microbiota by antibiotics protects the host from arsenic-induced inhibition of cholesterol synthesis, metabolism, and efflux, highlighting the role of gut microbiota as an important mediator of arsenic effects on cholesterol homeostasis.

In addition, serum cholesterol levels were significantly higher in 1 ppm arsenic-treated conventional mice (Figure 5A) than in controls. Since genes associated with cholesterol synthesis had low expression levels, the high levels of serum cholesterol should have mainly been caused by the relative low expression of *Ldlr* and *Scarb1* (Figure 4A). LDLR, encoded by the *Ldlr* gene, is the receptor for LDL (Go and Mani 2012), and SR-B1, encoded by the *Scarb1* gene, is the receptor for HDL (Trigatti et al. 2003). LDLR and SR-B1 conduct RCT, during which cholesterol is removed from circulation, and thus play important roles in cholesterol homeostasis (Ohashi et al. 2005; Tall 1998). Conversely, AB-treated mice exposed to 1 ppm arsenic had significantly lower serum cholesterol levels than the controls, which was consistent with the high expression levels of *Ldlr* and *Scarb1* (Figures 4B and 5B). High serum cholesterol levels are considered a risk factor for CVDs, as they are associated with high CVD morbidity and mortality rates (Stamler et al. 2000). Therefore, our data indicate that the effects of arsenic exposure on cholesterol homeostasis can be profoundly modified by the status of the gut microbiota, which may further influence disease outcomes due to exposure to arsenic and beyond.

In addition to the homeostasis of cholesterol, arsenic also influences lipid and fatty acid metabolism. According to previous studies, chronic arsenic exposure could disrupt lipid metabolism (Cheng et al. 2011) and improve TG levels in rat serum when coapplied with a high-cholesterol diet (Wang et al. 2015). In addition, arsenic exposure can induce lipid accumulation in macrophages in an *ApoE*$^{-/-}$ mouse model (Lemaire et al. 2014). Herein, our study also indicated that both serum and liver lipid homeostasis were largely perturbed in conventional mice exposed to 1 ppm arsenic (Figures 6 and 7). We found that the levels of multiple types of serum lipids were higher in 1 ppm arsenic-exposed mice than in control mice (Figure 6). The level of TGs was considerably higher (Figure 6). Because the serum TG level is regarded as a risk factor for CVDs, the high TG level may indicate that arsenic increases the risk of CVDs (Hokanson and Austin 1996). However, this effect was not observed in arsenic-exposed AB-treated mice, which, again, highlights the important role of the gut microbiota in the effects of arsenic exposure. Previous studies have revealed that the gut microbiota plays an important role in host lipid metabolism. For example, a previous study found bacteria-produced short-chain fatty acids played an important regulatory role in the balance among fatty acid synthesis, fatty acid oxidation, and lipolysis in the host body (den Besten et al. 2013). A germ-free mouse had a different lipid/fatty acid pattern in its liver, serum, and adipose tissue than a conventional mouse (Velagapudi et al. 2010). Another study also demonstrated that individual variations in the gut microbiota contribute to the differing blood lipid levels in humans (Fu et al. 2015). Thus, taken together, these previous studies and the study presented herein indicate that the status of the gut microbiota can profoundly modulate the effects of arsenic on lipid homeostasis.

This study provides evidence, based on an AB-treated mouse model, that the gut microbiota might attenuate or possibly reverse arsenic-induced LXR/RXR signaling inhibition and lipid/cholesterol dysbiosis. While the mechanism underlying these phenomena remain unclear, the data presented herein provide clues to how the gut microbiota influences the effects of arsenic on LXR/RXR signaling in the liver. First, gut microbiota–induced inflammation may play a key role in this process. A previous study showed that lipopolysaccharide (LPS) rapidly inhibited RXR proteins in the hamster liver (Beigneux et al. 2000). In addition, microbiota-induced intestinal inflammation can induce a retinoic acid deficiency, which may also influence the activation of RXR, since 9-*cis*-retinoic acid is an important endogenous ligand of RXR (Heyman et al. 1992). Consistent with these studies, we also found that the "LPS/IL-1 Mediated Inhibition of RXR Function" pathway was activated in arsenic-exposed conventional mice, whereas this pathway, as well as the "Acute Phase Response Signaling" pathway, was inhibited in mice treated with antibiotics (Figure 1B,C). Therefore, RXR inhibition could be a potential mechanism by which the gut microbiota affects arsenic-induced LXR/RXR inhibition. If this is true, we speculate that the gut microbiota-associated RXR inhibition would have impacts beyond LXR/RXR signaling, since RXR is required for multiple transcription factors, such as farnesoid X–activated receptor (FXR) (Grober et al. 1999), peroxisome proliferator–activated receptor alpha (Bardot et al. 1993), thyroid hormone receptor

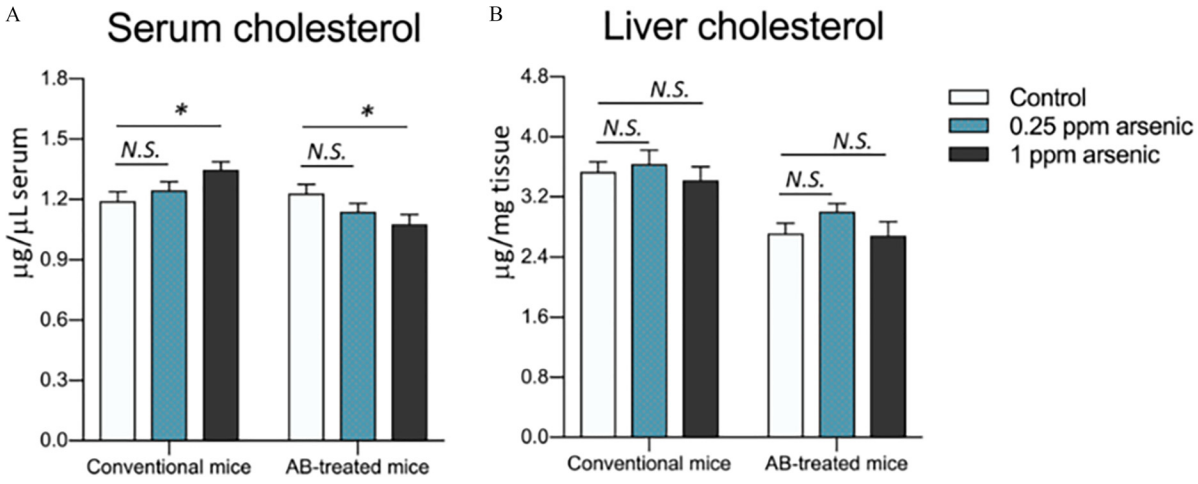

Figure 5. (A) Serum, and (B) hepatic cholesterol levels in conventional and antibiotic (AB)-treated mice. Mice treated with either water or 0.5 mg/mL cefoperazone were exposed to either vehicle, 0.25 ppm arsenic, or 1.0 ppm arsenic for 2 wk, after which mice were euthanized and serum and liver tissues were harvested. Cholesterol levels were measured by a cholesterol assay kit. $n = 10$ per group. N.S., no significant difference ($p > 0.05$); $^{*}p < 0.05$. Adjusted p-values were determined by two-way analysis of variance (ANOVA) Dunnett's multiple comparisons test.

(TR) (Castillo et al. 2004), pregnane X receptor (PXR) (Kliewer et al. 1998), and constitutive androstane receptor (Suino et al. 2004). Indeed, we found that the gene expression–associated various related pathways were different between arsenic-treated conventional animals and control mice, including "PXR/RXR activation" and "TR/RXR Activation" (Figure 1B). Second, bile acid conversion is a main source of cholesterol consumption, and bile acid–regulated FXR/RXR signaling also deeply influences LXR/RXR function as well as lipid and cholesterol homeostasis in the liver (Kalaany and Mangelsdorf 2006; Watanabe et al. 2004). Moreover, the gut microbiota is known to play a critical role in bile acid metabolism, and previous research revealed that the bile acid homeostasis in germ-free animals was largely different from those in conventional animals (Ridlon et al. 2014; Swann et al. 2011). Thus, it is possible that the gut microbiota mediates arsenic-induced lipid/cholesterol dysbiosis by mediating bile acid metabolism, thus influencing hepatic FXR/RXR signaling. Indeed, we also found that the gene encoding the rate-limiting enzyme CYP7A1 in bile acid synthesis was lower in arsenic-exposed conventional animals but higher in AB-treated mice exposed to arsenic (Figure 2C). On the

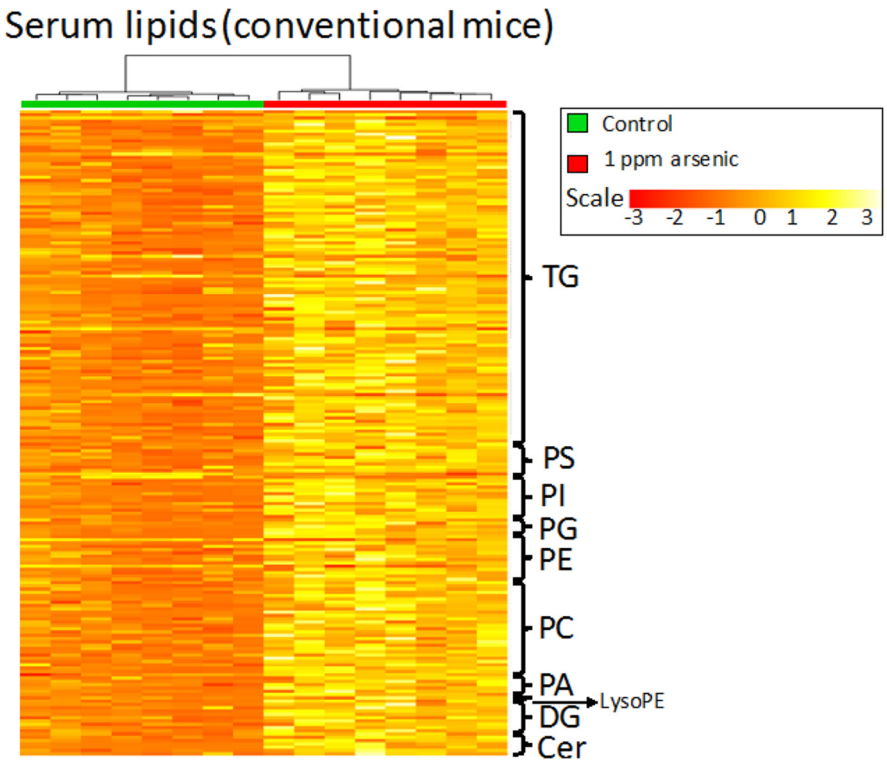

Figure 6. Histogram of serum lipid levels in conventional mice treated with vehicle or 1 ppm arsenic for 2 wk ($n = 8$ per group). For antibiotic (AB)-treated mice, no serum lipid has significant difference between controls and arsenic-treated mice. The scale was generated by autoscaling based on peak intensity. Note: Cer, ceramides; DG, diglyceride; lysoPE, lysophosphatidyl-ethanolamine; PA, phosphatidic acid; PC, phosphatidylcholine; PE, phosphatidylethanolamine; PG, phosphatidylglycerol; PI, phosphatidylinositol; PS, phosphatidylserine; TG, triglyceride.

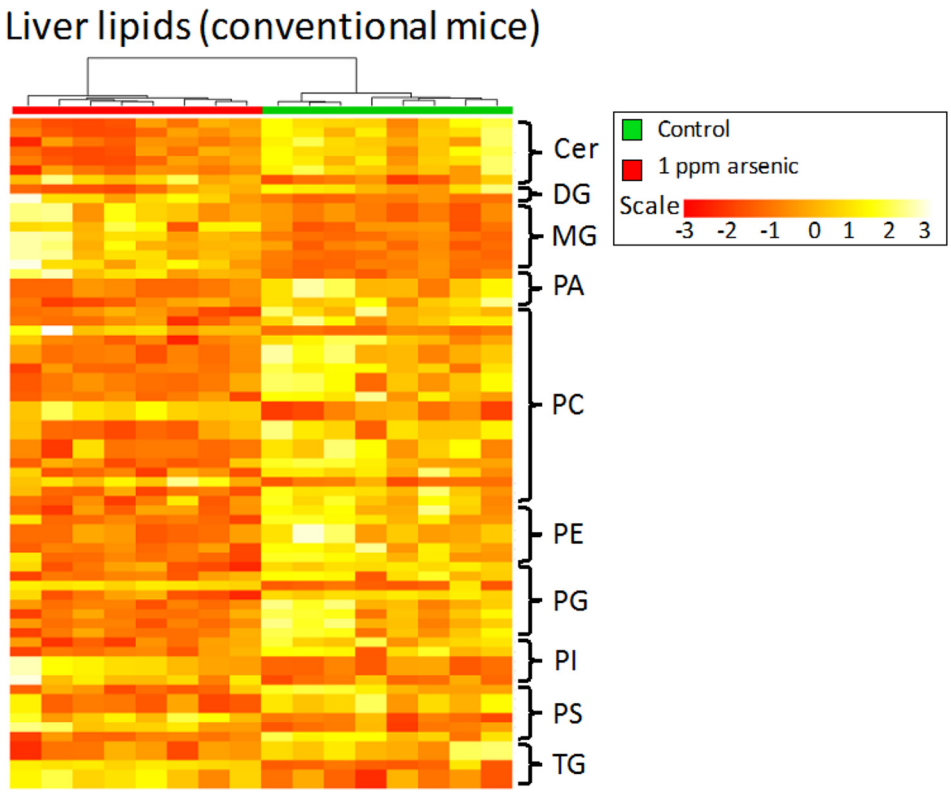

Figure 7. Histogram of hepatic lipid levels in conventional mice treated with vehicle or 1 ppm arsenic for 2 wk ($n = 8$ per group). For antibiotic (AB)-treated mice, no hepatic lipid has significant difference between controls and arsenic-treated mice. The scale was generated by autoscaling based on peak intensity. Cer, ceramides; DG, diglyceride; MG, monoacylglycerol; PA, phosphatidic acid; PC, phosphatidylcholine; PE, phosphatidylethanolamine; PG, phosphatidylglycerol; PI, phosphatidylinositol; PS, phosphatidylserine; TG, triglyceride.

other hand, our previous studies revealed that arsenic exposure can dramatically reshape the gut microbiota community and its metabolic functions (Chi et al. 2017; Lu et al. 2014a), thereby raising another possibility that arsenic exposure also influences bile acid homeostasis by disturbing the normal gut microbiota, resulting in lipid and cholesterol dysbiosis. However, our current understanding of the effect of arsenic exposure on bile acid homeostasis and whether the gut microbiota plays a role in this effect is still limited and needs to be explored in the future.

Our current study has several limitations. First, as a proof of principle study, to ensure the AB-treated mice were maintained in a good gut microbiota–depleting condition, we performed the 2-wk arsenic treatment, which is an acute exposure. However, arsenic exposure in humans is generally chronic. Therefore, how chronic arsenic exposure affects hepatic LXR/RXR signaling and whether gut microbiota plays a regulating role in this process still need to be further explored. Second, although we used environmentally relevant dose levels in this study, considering the

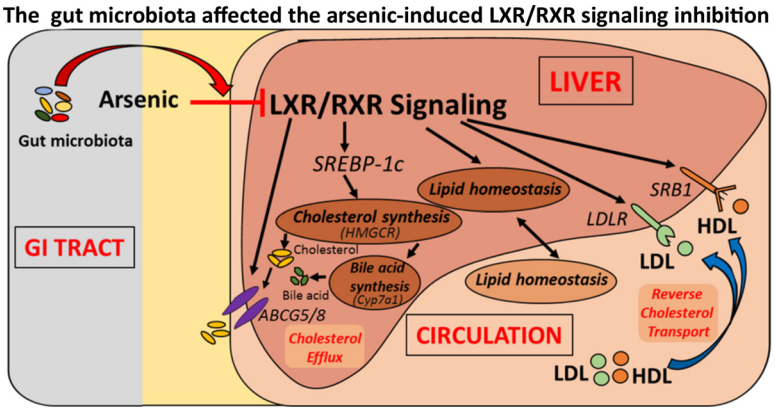

Figure 8. A proposed diagram shows how gut microbiota affected the arsenic effects on liver X receptor/retinoid X receptor (LXR/RXR) pathways. The gut microbiota status affected the effects of arsenic on hepatic LXR/RXR signaling and thus might further affect lipid and cholesterol homeostasis. In mice with the normal gut microbiota, arsenic exposure inhibited the LXR/RXR signaling in the liver; disturbed the cholesterol synthesis, efflux, and absorption; and also affected the lipid homeostasis in liver and circulation. However, gut microbiota disruption attenuated or even reversed the effects of arsenic exposure on hepatic LXR/RXR signaling as well as the lipid and cholesterol homeostasis. *ABCG5/8*, ATP binding cassette subfamily G member 5/8; *CYP7A1*, cytochrome P450 family 7 subfamily A member 1; GI, gastrointestinal tract; HDL, high-density lipoprotein; *HMGCR*, 3-hydroxy-3-methylglutaryl-CoA reductase; LDL, low-density lipoprotein; *LDLR*, low-density lipoprotein receptor; *SRB1*, scavenger receptor class B member 1; *SREBP-1c*, sterol regulatory element-binding protein 1.

relatively short exposure period and the mouse model we used, which requires a higher dose to reach the human-equivalent dose in the body (Nair and Jacob 2016), some of our analysis included both 0.25 ppm and 1 ppm exposure groups. Future study is warranted to explore the effects of arsenic exposure at more human-relevant low doses below 0.1 ppm. Third, this study only used female mice, mainly because it has been well established in our previous studies that arsenic disrupted the normal gut microbiota compositions and their metabolic profiles in female mice, as well as their interactions with the host. However, sex is a critical factor in arsenic susceptibility (Bardullas et al. 2009), and our previous study found that arsenic and other environmental chemicals differently perturbed gut microbiota in female and male mice (Chi et al. 2016; Gao et al. 2017). Future studies are needed to elucidate the role of sex in exposure–microbiota–host interactions. Finally, gut microbiota has complex and far-reaching roles that affect numerous physiological processes in host bodies. We used antibiotics to treat mice, trying to generate mice with depleted gut microbiota. Our data show arsenic differentially altered lipid and cholesterol homeostasis in controls and mice treated with antibiotics, suggesting the potential role of the gut microbiota in these processes. However, the complicated effects of antibiotic treatment on host bodies could not be completely ruled out and need to be addressed in the future.

In conclusion, this study provides evidence in an AB-treated mouse model that the status of the gut microbiota can modify the effects of arsenic exposure on cholesterol and lipid homeostasis (Figure 8). Arsenic exposure suppressed the expression of multiple genes involved in cholesterol synthesis, metabolism, and transportation in conventional mice but not in AB-treated mice. Moreover, serum cholesterol concentrations were oppositely regulated by arsenic in mice depending on the gut microbiota. The influence of arsenic exposure on liver and serum lipid homeostasis was also much smaller in AB-treated mice than in conventional mice. Our findings elucidate a new factor underlying the effects of arsenic on cholesterol and lipid metabolism and suggest that arsenic-induced cardiovascular effects may be attenuated by modulating the gut microbiota.

Acknowledgments

This work was support in part by a National Institutes of Health (NIH) grant (R01ES024950) and the University of North Carolina Center for Environmental Health and Susceptibility with the NIH grant (P30ES010126).

References

Adebayo AO, Zandbergen F, Kozul-Horvath CD, Gruppuso PA, Hamilton JW. 2015. Chronic exposure to low-dose arsenic modulates lipogenic gene expression in mice. J Biochem Mol Toxicol 29(1):1–9, PMID: 25155036, https://doi.org/10.1002/jbt.21600.

al-Waiz M, Mikov M, Mitchell S, Smith RL. 1992. The exogenous origin of trimethylamine in the mouse. Metab Clin Exp 41(2):135–136, PMID: 1736035, https://doi.org/10.1016/0026-0495(92)90140-6.

Antonopoulos DA, Huse SM, Morrison HG, Schmidt TM, Sogin ML, Young VB. 2009. Reproducible community dynamics of the gastrointestinal microbiota following antibiotic perturbation. Infect Immun 77(6):2367–2375, PMID: 19307217, https://doi.org/10.1128/IAI.01520-08.

Attie AD. 2007. ABCA1: at the nexus of cholesterol, HDL and atherosclerosis. Trends Biochem Sci 32(4):172–179, PMID: 17324574, https://doi.org/10.1016/j.tibs.2007.02.001.

Auken G. 1945. The influence of the administration of arsenic on serum cholesterol. Acta Pharmacol Toxicol (Copenh) 1:369–378, https://doi.org/10.1111/j.1600-0773.1945.tb02590.x.

Bardot O, Aldridge TC, Latruffe N, Green S. 1993. PPAR-RXR heterodimer activates a peroxisome proliferator response element upstream of the bifunctional enzyme gene. Biochem Biophys Res Commun 192(1):37–45, PMID: 8386511, https://doi.org/10.1006/bbrc.1993.1378.

Bardullas U, Limón-Pacheco J, Giordano M, Carrizales L, Mendoza-Trejo M, Rodríguez V. 2009. Chronic low-level arsenic exposure causes gender-specific alterations in locomotor activity, dopaminergic systems, and thioredoxin expression in mice. Toxicol Appl Pharmacol 239(2):169–177, PMID: 19121333, https://doi.org/10.1016/j.taap.2008.12.004.

Beigneux AP, Moser AH, Shigenaga JK, Grunfeld C, Feingold KR. 2000. The acute phase response is associated with retinoid X receptor repression in rodent liver. J Biol Chem 275(21):16390–16399, PMID: 10747970, https://doi.org/10.1074/jbc.M000953200.

Berg M, Tran HC, Nguyen TC, Pham HV, Schertenleib R, Giger W. 2001. Arsenic contamination of groundwater and drinking water in Vietnam: a human health threat. Environ Sci Technol 35(13):2621–2626, PMID: 11452583, https://doi.org/10.1021/es010027y.

Caesar R, Fåk F, Bäckhed F. 2010. Effects of gut microbiota on obesity and atherosclerosis via modulation of inflammation and lipid metabolism. J Intern Med 268(4):320–328, PMID: 21050286, https://doi.org/10.1111/j.1365-2796.2010.02270.x.

Castillo AI, Sánchez-Martínez R, Moreno JL, Martínez-Iglesias OA, Palacios D, Aranda A. 2004. A permissive retinoid X receptor/thyroid hormone receptor heterodimer allows stimulation of prolactin gene transcription by thyroid hormone and 9-cis-retinoic acid. Mol Cell Biol 24(2):502–513, PMID: 14701725, https://doi.org/10.1128/mcb.24.2.502-513.2004.

Chen Y, Graziano JH, Parvez F, Liu M, Slavkovich V, Kalra T, et al. 2011. Arsenic exposure from drinking water and mortality from cardiovascular disease in Bangladesh: prospective cohort study. BMJ 342:d2431, PMID: 21546419, https://doi.org/10.1136/bmj.d2431.

Cheng TJ, Chuu JJ, Chang CY, Tsai WC, Chen KJ, Guo HR. 2011. Atherosclerosis induced by arsenic in drinking water in rats through altering lipid metabolism. Toxicol Appl Pharmacol 256(2):146–153, PMID: 21851829, https://doi.org/10.1016/j.taap.2011.08.001.

Chi L, Bian X, Gao B, Ru H, Tu P, Lu K. 2016. Sex-specific effects of arsenic exposure on the trajectory and function of the gut microbiome. Chem Res Toxicol 29(6):949–951, PMID: 27268458, https://doi.org/10.1021/acs.chemrestox.6b00066.

Chi L, Bian X, Gao B, Tu P, Ru H, Lu K. 2017. The effects of an environmentally relevant level of arsenic on the gut microbiome and its functional metagenome. Toxicol Sci 160(2):193–204, PMID: 28973555, https://doi.org/10.1093/toxsci/kfx174.

Chi L, Xue J, Tu P, Lai Y, Ru H, Lu K. 2018. Gut microbiome disruption altered the biotransformation and liver toxicity of arsenic in mice. Arch Toxicol 93(1):25–35, PMID: 30357543, https://doi.org/10.1007/s00204-018-2332-7.

Chiang JY, Kimmel R, Stroup D. 2001. Regulation of cholesterol 7α-hydroxylase gene (CYP7A1) transcription by the liver orphan receptor (LXRα). Gene 262(1–2):257–265, PMID: 11179691, https://doi.org/10.1016/s0378-1119(00)00518-7.

Chowdhury UK, Biswas BK, Chowdhury TR, Samanta G, Mandal BK, Basu GC, et al. 2000. Groundwater arsenic contamination in Bangladesh and West Bengal, India. Environ Health Perspect 108(5):393–397, PMID: 10811564, https://doi.org/10.1289/ehp.00108393.

Cui X, Wakai T, Shirai Y, Hatakeyama K, Hirano S. 2006. Chronic oral exposure to inorganic arsenate interferes with methylation status of p16ink4a and RASSF1A and induces lung cancer in A/J mice. Toxicol Sci 91(2):372–381, PMID: 16543296, https://doi.org/10.1093/toxsci/kfj159.

den Besten G, van Eunen K, Groen AK, Venema K, Reijngoud DJ, Bakker BM. 2013. The role of short-chain fatty acids in the interplay between diet, gut microbiota, and host energy metabolism. J Lipid Res 54(9):2325–2340, PMID: 23821742, https://doi.org/10.1194/jlr.R036012.

Fu J, Bonder MJ, Cenit MC, Tigchelaar EF, Maatman A, Dekens JA, et al. 2015. The gut microbiome contributes to a substantial proportion of the variation in blood lipids. Circ Res 117(9):817–824, PMID: 26358192, https://doi.org/10.1161/CIRCRESAHA.115.306807.

Gao B, Bian X, Mahbub R, Lu K. 2017. Gender-specific effects of organophosphate diazinon on the gut microbiome and its metabolic functions. Environ Health Perspect 125(2):198–206, PMID: 27203275, https://doi.org/10.1289/EHP202.

Go GW, Mani A. 2012. Low-density lipoprotein receptor (LDLR) family orchestrates cholesterol homeostasis. Yale J Biol Med 85(1):19–28, PMID: 22461740.

Grober J, Zaghini I, Fujii H, Jones SA, Kliewer SA, Willson TM, et al. 1999. Identification of a bile acid-responsive element in the human ileal bile acid-binding protein gene. Involvement of the farnesoid x receptor/9-cis-retinoic acid receptor heterodimer. J Biol Chem 274(42):29749–29754, PMID: 10514450, https://doi.org/10.1074/jbc.274.42.29749.

Heyman RA, Mangelsdorf DJ, Dyck JA, Stein RB, Eichele G, Evans RM, et al. 1992. 9-cis retinoic acid is a high affinity ligand for the retinoid x receptor. Cell 68(2):397–406, PMID: 1310260, https://doi.org/10.1016/0092-8674(92)90479-v.

Hokanson JE, Austin MA. 1996. Plasma triglyceride level is a risk factor for cardiovascular disease independent of high-density lipoprotein cholesterol level: a meta-analysis of population-based prospective studies. J Cardiovasc Risk 3(2):213–219, PMID: 8836866, https://doi.org/10.1097/00043798-199604000-00014.

Hong Y, Piao F, Zhao Y, Li S, Wang Y, Liu P. 2009. Subchronic exposure to arsenic decreased Sdha expression in the brain of mice. Neurotoxicology 30(4):538–543, PMID: 19422848, https://doi.org/10.1016/j.neuro.2009.04.011.

Jandhyala SM, Talukdar R, Subramanyam C, Vuyyuru H, Sasikala M, Reddy DN. 2015. Role of the normal gut microbiota. World J Gastroenterol 21(29):8787–8803, PMID: 26269668, https://doi.org/10.3748/wjg.v21.i29.8787.

Joseph SB, Laffitte BA, Patel PH, Watson MA, Matsukuma KE, Walczak R, et al. 2002a. Direct and indirect mechanisms for regulation of fatty acid synthase gene expression by liver x receptors. J Biol Chem 277(13):11019–11025, PMID: 11790787, https://doi.org/10.1074/jbc.M111041200.

Joseph SB, McKilligin E, Pei L, Watson MA, Collins AR, Laffitte BA, et al. 2002b. Synthetic LXR ligand inhibits the development of atherosclerosis in mice. Proc Natl Acad Sci USA 99(11):7604–7609, PMID: 12032330, https://doi.org/10.1073/pnas.112059299.

Kalaany NY, Mangelsdorf DJ. 2006. LXRs and FXR: the yin and yang of cholesterol and fat metabolism. Annu Rev Physiol 68:159–191, PMID: 16460270, https://doi.org/10.1146/annurev.physiol.68.033104.152158.

Kim D, Langmead B, Salzberg SL. 2015. HISAT: a fast spliced aligner with low memory requirements. Nat Methods 12(4):357–360, PMID: 25751142, https://doi.org/10.1038/nmeth.3317.

Kliewer SA, Moore JT, Wade L, Staudinger JL, Watson MA, Jones SA, et al. 1998. An orphan nuclear receptor activated by pregnanes defines a novel steroid signaling pathway. Cell 92(1):73–82, PMID: 9489701, https://doi.org/10.1016/s0092-8674(00)80900-9.

Koeth RA, Wang Z, Levison BS, Buffa JA, Org E, Sheehy BT, et al. 2013. Intestinal microbiota metabolism of L-carnitine, a nutrient in red meat, promotes atherosclerosis. Nat Med 19(5):576, PMID: 23563705, https://doi.org/10.1038/nm.3145.

Lemaire M, Lemarie CA, Flores Molina M, Guilbert C, Lehoux S, Mann KK. 2014. Genetic deletion of LXRα prevents arsenic-enhanced atherosclerosis, but not arsenic-altered plaque composition. Toxicol Sci 142(2):477–488, PMID: 25273567, https://doi.org/10.1093/toxsci/kfu197.

Lemaire M, Lemarié CA, Flores Molina M, Schiffrin EL, Lehoux S, Mann KK. 2011. Exposure to moderate arsenic concentrations increases atherosclerosis in ApoE−/− mouse model. Toxicol Sci 122(1):211–221, PMID: 21512104, https://doi.org/10.1093/toxsci/kfr097.

Lu K, Abo RP, Schlieper KA, Graffam ME, Levine S, Wishnok JS, et al. 2014a. Arsenic exposure perturbs the gut microbiome and its metabolic profile in mice: an integrated metagenomics and metabolomics analysis. Environ Health Perspect 122(3):284–291, PMID: 24413286, https://doi.org/10.1289/ehp.1307429.

Lu K, Mahbub R, Cable PH, Ru H, Parry NM, Bodnar WM, et al. 2014b. Gut microbiome phenotypes driven by host genetics affect arsenic metabolism. Chem Res Toxicol 27(2):172–174, PMID: 24490651, https://doi.org/10.1021/tx400454z.

Matyash V, Liebisch G, Kurzchalia TV, Shevchenko A, Schwudke D. 2008. Lipid extraction by methyl-tert-butyl ether for high-throughput lipidomics. J Lipid Res 49(5):1137–1146, PMID: 18281723, https://doi.org/10.1194/jlr.D700041-JLR200.

Mutemberezi V, Guillemot-Legris O, Muccioli GG. 2016. Oxysterols: from cholesterol metabolites to key mediators. Prog Lipid Res 64:152–169, PMID: 27687912, https://doi.org/10.1016/j.plipres.2016.09.002.

Nair AB, Jacob S. 2016. A simple practice guide for dose conversion between animals and human. J Basic Clin Pharm 7(2):27–31, PMID: 27057123, https://doi.org/10.4103/0976-0105.177703.

Naujokas MF, Anderson B, Ahsan H, Aposhian HV, Graziano JH, Thompson C, et al. 2013. The broad scope of health effects from chronic arsenic exposure: update on a worldwide public health problem. Environ Health Perspect 121(3):295–302, PMID: 23458756, https://doi.org/10.1289/ehp.1205875.

Navas-Acien A, Sharrett AR, Silbergeld EK, Schwartz BS, Nachman KE, Burke TA, et al. 2005. Arsenic exposure and cardiovascular disease: a systematic review of the epidemiologic evidence. Am J Epidemiol 162(11):1037–1049, PMID: 16269585, https://doi.org/10.1093/aje/kwi330.

Nicholson JK, Holmes E, Kinross J, Burcelin R, Gibson G, Jia W, et al. 2012. Host-gut microbiota metabolic interactions. Science 336(6086):1262–1267, PMID: 22674330, https://doi.org/10.1126/science.1223813.

Ohashi R, Mu H, Wang X, Yao Q, Chen C. 2005. Reverse cholesterol transport and cholesterol efflux in atherosclerosis. QJM 98(12):845–856, PMID: 16258026, https://doi.org/10.1093/qjmed/hci136.

Padovani AM, Molina MF, Mann KK. 2010. Inhibition of liver X receptor/retinoid X receptor–mediated transcription contributes to the proatherogenic effects of arsenic in macrophages in vitro. Arterioscler Thromb Vasc Biol 30(6):1228–1236, PMID: 20339114, https://doi.org/10.1161/ATVBAHA.110.205500.

Pandak WM, Schwarz C, Hylemon PB, Mallonee D, Valerie K, Heuman DM, et al. 2001. Effects of CYP7A1 overexpression on cholesterol and bile acid homeostasis. Am J Physiol Gastrointest Liver Physiol 281(4):G878–G889, PMID: 11557507, https://doi.org/10.1152/ajpgi.2001.281.4.G878.

Peet DJ, Turley SD, Ma W, Janowski BA, Lobaccaro JM, Hammer RE, et al. 1998. Cholesterol and bile acid metabolism are impaired in mice lacking the nuclear oxysterol receptor LXRα. Cell 93(5):693–704, PMID: 9630215, https://doi.org/10.1016/s0092-8674(00)81432-4.

Repa JJ, Liang G, Ou J, Bashmakov Y, Lobaccaro J-M, Shimomura I, et al. 2000. Regulation of mouse sterol regulatory element-binding protein-1c gene (SREBP-1c) by oxysterol receptors, LXRα and LXRβ. Genes Dev 14(22):2819–2830, PMID: 11090130, https://doi.org/10.1101/gad.844900.

Ridlon JM, Kang DJ, Hylemon PB, Bajaj JS. 2014. Bile acids and the gut microbiome. Curr Opin Gastroenterol 30(3):332–338, PMID: 24625896, https://doi.org/10.1097/MOG.0000000000000057.

Romano KA, Vivas EI, Amador-Noguez D, Rey FE. 2015. Intestinal microbiota composition modulates choline bioavailability from diet and accumulation of the proatherogenic metabolite trimethylamine-N-oxide. MBio 6(2):e02481, PMID: 25784704, https://doi.org/10.1128/mBio.02481-14.

Rubin SSD, Alava P, Zekker I, Du Laing G, Van de Wiele T. 2014. Arsenic thiolation and the role of sulfate-reducing bacteria from the human intestinal tract. Environ Health Perspect 122(8):817–822, PMID: 24833621, https://doi.org/10.1289/ehp.1307759.

Scripps Research. Metlin Database. https://metlin.scripps.edu/landing_page.php?pgcontent=mainPage [accessed 29 January 2018].

Sharpe LJ, Brown AJ. 2013. Controlling cholesterol synthesis beyond 3-hydroxy-3-methylglutaryl-CoA reductase (HMGCR). J Biol Chem 288(26):18707–18715, PMID: 23696639, https://doi.org/10.1074/jbc.R113.479808.

Shimano H. 2001. Sterol regulatory element-binding proteins (SREBPs): transcriptional regulators of lipid synthetic genes. Prog Lipid Res 40(6):439–452, PMID: 11591434, https://doi.org/10.1016/S0163-7827(01)00010-8.

Simeonova PP, Hulderman T, Harki D, Luster MI. 2003. Arsenic exposure accelerates atherogenesis in apolipoprotein E (−/−) mice. Environ Health Perspect 111(14):1744, PMID: 14594625, https://doi.org/10.1289/ehp.6332.

Simeonova PP, Luster MI. 2004. Arsenic and atherosclerosis. Toxicol Appl Pharmacol 198(3):444–449, PMID: 15276425, https://doi.org/10.1016/j.taap.2003.10.018.

Singh A. 2004. Arsenic contamination in groundwater of North Eastern India. In: *Proceedings of the 11th National Symposium on Hydrology with Focal Theme on Water Quality*. Jain CK, Trivedi RC, Sharma KD, eds. 22–23 November 2004. Roorkee, India: National Institute of Hydrology, 255–262.

Stamler J, Daviglus ML, Garside DB, Dyer AR, Greenland P, Neaton JD. 2000. Relationship of baseline serum cholesterol levels in 3 large cohorts of younger men to long-term coronary, cardiovascular, and all-cause mortality and to longevity. JAMA 284(3):311–318, PMID: 10891962, https://doi.org/10.1001/jama.284.3.311.

States JC, Srivastava S, Chen Y, Barchowsky A. 2009. Arsenic and cardiovascular disease. Toxicol Sci 107(2):312–323, PMID: 19015167, https://doi.org/10.1093/toxsci/kfn236.

Straub AC, Stolz DB, Vin H, Ross MA, Soucy NV, Klei LR, et al. 2007. Low level arsenic promotes progressive inflammatory angiogenesis and liver blood vessel remodeling in mice. Toxicol Appl Pharmacol 222(3):327–336, PMID: 17123562, https://doi.org/10.1016/j.taap.2006.10.011.

Suino K, Peng L, Reynolds R, Li Y, Cha JY, Repa JJ, et al. 2004. The nuclear xenobiotic receptor car: structural determinants of constitutive activation and heterodimerization. Mol Cell 16(6):893–905, PMID: 15610733, https://doi.org/10.1016/j.molcel.2004.11.036.

Swann JR, Want EJ, Geier FM, Spagou K, Wilson ID, Sidaway JE, et al. 2011. Systemic gut microbial modulation of bile acid metabolism in host tissue compartments. Proc Natl Acad Sci USA 108(Suppl 1):4523–4530, PMID: 20837534, https://doi.org/10.1073/pnas.1006734107.

Tall AR. 1998. An overview of reverse cholesterol transport. Eur Heart J 19:A31–A35, PMID: 9519340.

Theriot CM, Bowman AA, Young VB. 2016. Antibiotic-induced alterations of the gut microbiota alter secondary bile acid production and allow for Clostridium difficile spore germination and outgrowth in the large intestine. MSphere 1(1):e00045–e00015, PMID: 27239562, https://doi.org/10.1128/mSphere.00045-15.

Trapnell C, Williams BA, Pertea G, Mortazavi A, Kwan G, Van Baren MJ, et al. 2010. Transcript assembly and quantification by RNA-Seq reveals unannotated transcripts and isoform switching during cell differentiation. Nat Biotechnol 28(5):511–515, PMID: 20436464, https://doi.org/10.1038/nbt.1621.

Trigatti BL, Krieger M, Rigotti A. 2003. Influence of the HDL receptor SR-BI on lipoprotein metabolism and atherosclerosis. Arterioscler Thromb Vasc Biol 23(10):1732–1738, PMID: 12920050, https://doi.org/10.1161/01.ATV.0000091363.28501.84.

Ulven SM, Dalen KT, Gustafsson JÅ, Nebb HI. 2005. LXR is crucial in lipid metabolism. Prostaglandins Leukot Essent Fatty Acids 73(1):59–63, https://doi.org/10.1016/j.plefa.2005.04.009.

Velagapudi VR, Hezaveh R, Reigstad CS, Gopalacharyulu P, Yetukuri L, Islam S, et al. 2010. The gut microbiota modulates host energy and lipid metabolism in mice. J Lipid Res 51(5):1101–1112, PMID: 20040631, https://doi.org/10.1194/jlr.M002774.

Wang Z, Klipfell E, Bennett BJ, Koeth R, Levison BS, Dugar B, et al. 2011. Gut flora metabolism of phosphatidylcholine promotes cardiovascular dis-

ease. Nature 472(7341):57–63, PMID: 21475195, https://doi.org/10.1038/nature09922.

Wang X, Mu X, Zhang J, Huang Q, Alamdar A, Tian M, et al. 2015. Serum metabolomics reveals that arsenic exposure disrupted lipid and amino acid metabolism in rats: a step forward in understanding chronic arsenic toxicity. Metallomics 7(3):544–552, PMID: 25697676, https://doi.org/10.1039/c5mt00002e.

Watanabe M, Houten SM, Wang L, Moschetta A, Mangelsdorf DJ, Heyman RA, et al. 2004. Bile acids lower triglyceride levels via a pathway involving FXR, SHP, and SREBP-1c. J Clin Invest 113(10):1408–1418, PMID: 15146238, https://doi.org/10.1172/JCI21025.

Willy PJ, Umesono K, Ong ES, Evans RM, Heyman RA, Mangelsdorf DJ. 1995. LXR, a nuclear receptor that defines a distinct retinoid response pathway. Genes Dev 9(9):1033–1045, PMID: 7744246, https://doi.org/10.1101/gad.9.9.1033.

Yu XH, Qian K, Jiang N, Zheng XL, Cayabyab FS, Tang CK. 2014. ABCG5/ABCG8 in cholesterol excretion and atherosclerosis. Clin Chim Acta 428:82–88, PMID: 24252657, https://doi.org/10.1016/j.cca.2013.11.010.

Zhang Y, Mangelsdorf DJ. 2002. LuXuRies of lipid homeostasis: the unity of nuclear hormone receptors, transcription regulation, and cholesterol sensing. Mol Interv 2(2):78–87, PMID: 14993353, https://doi.org/10.1124/mi.2.2.78.